AD-A125 040 THE POST-PROCESSING APPROACH IN THE FINITE ELEMENT METHOD PART 2 THE CALC..(U) MARYLAND UNIV COLLEGE PARK LAB FOR NUMERICAL ANALYSIS I BABUSKA ET AL. DEC 82 1/1

UNCLASSIFIED BN-993 N00014-77-C-0623 F/G 2/1. NL

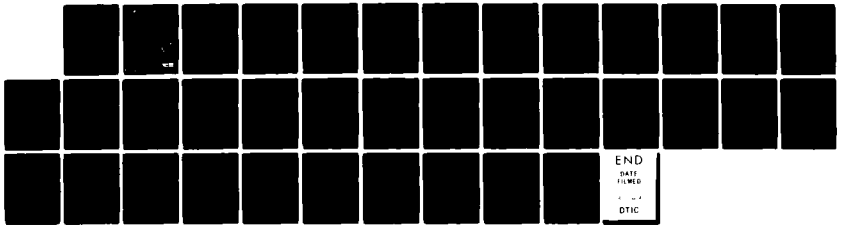

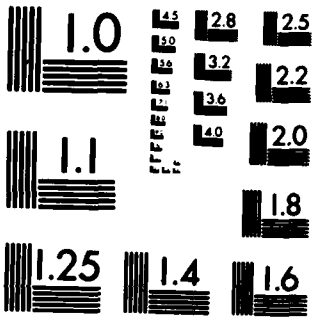

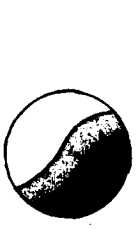

INSTITUTE FOR PHYSICAL SCIENCE
AND TECHNOLOGY

(15)

Laboratory for Numerical Analysis

Technical Note BN-993

THE POST-PROCESSING APPROACH IN THE FINITE ELEMENT METHOD
PART 2: THE CALCULATION OF STRESS INTENSITY FACTORS

BY

I. Babuška and A. Miller

December 1982

UNIVERSITY OF MARYLAND

SECURITY CLASSIFICATION OF THIS PAGE (When Data Entered)

REPORT DOCUMENTATION PAGE	READ INSTRUCTIONS BEFORE COMPLETING FORM
1. REPORT NUMBER: Technical Note BN-993 — 2. GOVT ACCESSION NO. A125040	3. RECIPIENT'S CATALOG NUMBER
4. TITLE (and Subtitle) THE POST-PROCESSING APPROACH IN THE FINITE ELEMENT METHOD. PART 2: THE CALCULATION OF STRESS INTENSITY FACTORS	5. TYPE OF REPORT & PERIOD COVERED Final-life of the contract
	6. PERFORMING ORG. REPORT NUMBER
7. AUTHOR(s) I. Babuška and A. Miller	8. CONTRACT OR GRANT NUMBER(s) ONR N00014-77-C-0623
9. PERFORMING ORGANIZATION NAME AND ADDRESS Institute for Physical Science and Technology, University of Maryland, College Park, MD 20742	10. PROGRAM ELEMENT, PROJECT, TASK AREA & WORK UNIT NUMBERS
11. CONTROLLING OFFICE NAME AND ADDRESS Department of the Navy, Office of Naval Research, Arlington, VA 22217	12. REPORT DATE December 1982
	13. NUMBER OF PAGES 32
14. MONITORING AGENCY NAME & ADDRESS(if different from Controlling Office)	15. SECURITY CLASS. (of this report)
	15a. DECLASSIFICATION/DOWNGRADING SCHEDULE

16. DISTRIBUTION STATEMENT (of this Report)

Approved for public release: distribution unlimited

17. DISTRIBUTION STATEMENT (of the abstract entered in Block 20, if different from Report)

18. SUPPLEMENTARY NOTES

19. KEY WORDS (Continue on reverse side if necessary and identify by block number)

20. ABSTRACT (Continue on reverse side if necessary and identify by block number)

In the context of a model problem we describe post-processing techniques for the calculation of generalized stress intensity factors. We discuss two broad classes of methods, one involving an "influence" function, and the other related to the well-known energy release principle of fracture mechanics. An error analysis is sketched and two numerical examples are given to illustrate the effectivity of the techniques.

DD FORM 1 JAN 73 1473 EDITION OF 1 NOV 65 IS OBSOLETE

S/N 0102-LF-014-6601

SECURITY CLASSIFICATION OF THIS PAGE (When Data Entered)

THE POST-PROCESSING APPROACH IN THE FINITE ELEMENT METHOD

PART 2: THE CALCULATION OF STRESS INTENSITY FACTORS

BY

I. BABUŠKA AND A. MILLER

Technical Note BN-993

This research was partially supported by ONR Contract N00014-77-C-0623. The computations were carried out with support from the Computer Science Center of the University of Maryland, College Park.

Abstract

In the context of a model problem ~~we~~ the authors describe post-processing techniques for the calculation of generalized stress intensity factors. ~~We~~ They discuss two broad classes of methods, one involving an "influence" function, and the other related to the well-known energy release principle of fracture mechanics. An error analysis is sketched and two numerical examples are give to illustrate the effectivity of the techniques.

This is the second in a series of papers.

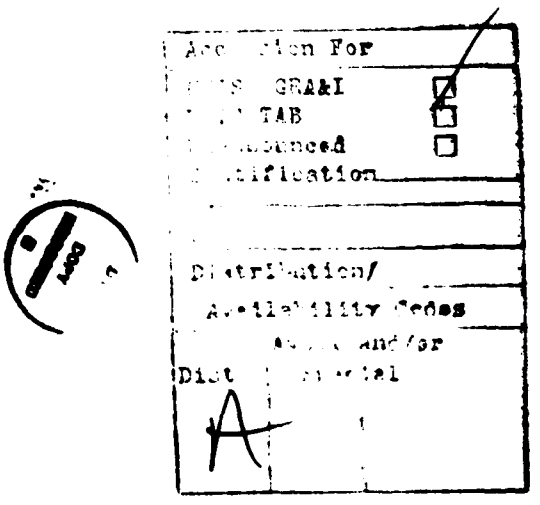

§1. Introduction

§1.1. General Introduction

This is the second in a series of three papers in which we discuss "post-processing" as it may be applied in the finite element method. In the first paper [1] we briefly described some general aspects of post-processing, and illustrated a few of the ideas in the particular cases of two model problems from structural mechanics. For these model problems we were concerned with obtaining values for the displacements, stresses, bending moments etc., either at a point or as an average over some subsection of the structure. However, we were careful to note that for two dimensional problems the methods discussed could only be expected to perform well if the point or subsection under consideration was "reasonably distant" from any corner point of the region occupied by the structure. In this paper we take up the problem of how to proceed when this "reasonably distant" criterion is no longer satisfied.

As is well known, corner points usually give rise to some form of singular behavior in the derivatives of the displacements. In fact, the stress intensity factors of elasticity theory are the coefficients of the terms that exhibit this singular behavior. They serve as a means of characterizing the state of stress in the neighborhood of the corner point. We shall see that calculation of these stress intensity factors, as well as certain coefficients of non-singular terms, is possible within the post-processing scheme. If desired, values of the displacements or stresses at points near the corner may then be found by using

the values of the stress intensity factors, along with the non-singular coefficients, in known asymptotic expansions valid in the vicinity of the corner point.

In this paper our post-processing calculations will be based on expressions that are of a slightly more general form than those dealt with in the first paper of this series. In place of the model expression for the generic quantity Φ which appears there (see (1.1) of [1]), we will now consider expressions for Φ which take the form

$$(1.1)\quad \Phi = \Phi(\omega) = \int_\Omega \lambda \cdot \nabla\omega dA + \int_\Omega \xi\omega dA + \int_{\partial\Omega} \rho\omega ds + R,$$

where $\lambda = (\lambda_1, \lambda_2)$ is a vector function on Ω, ξ is a scalar function on Ω, ρ is a scalar function defined on $\partial\Omega$, or some specified portion of $\partial\Omega$, and R is an integral which is easily computable from the load data of the problem. If $\tilde{\omega}$ is a finite element approximation to ω, then (1.1) suggests that we use

$$(1.2)\quad \tilde{\Phi} = \tilde{\Phi}(\tilde{\omega}) = \int_\Omega \lambda \cdot \nabla\tilde{\omega} dA + \int_\Omega \xi\tilde{\omega} dA + \int_{\partial\Omega} \rho\tilde{\omega} ds + R$$

as an approximation to Φ (c.f. (1.2) of [1]).

§1.2. Formulation of the model problem

As usual, we shall describe the post-processing technique in the context of a particular model problem. Suppose Ω is a bounded, two dimensional region whose boundary is made up of smooth arcs $\Gamma_1, \ldots, \Gamma_s$. Consider a boundary value problem governed by the equation

(1.3a) $$\nabla^2\omega = 0 \quad \text{in} \quad \Omega,$$

and for which, independently on each Γ_j, either the Dirichlet boundary condition

(1.3b) $$\omega = f_j \quad \text{on} \quad \Gamma_j$$

or the Neumann boundary condition

(1.3c) $(\nabla\omega)\cdot\hat{n} = g_j$ on Γ_j ($\hat{n}$ = outward pointing unit normal)

applies. For definiteness, assume that Γ_1 and Γ_2 are adjacent edges of Ω which meet at the origin of the coordinate system (x_1,x_2). Establish polar coordinates (r,θ) at this origin, and suppose that Γ_1 and Γ_2 are in fact straight line segments which correspond to $\theta = 0$ and $\theta = \alpha\pi$ respectively. Assume that in the vicinity of 0 the region Ω corresponds to the cone $0 < \theta < \alpha\pi$ (see Figure 1). For Γ_1 and Γ_2, let the boundary conditions (1.3b) and (1.3c) take the specific form

(1.3d) $\omega = f_1 = 0$ on Γ_1, and $(\nabla\omega)\cdot\hat{n} = g_2 = 0$ on Γ_2.

(If $\alpha = 2$, then what we have described models a slit domain. The upper face ($\theta = 0$) of the slit is fixed, whereas the lower face ($\theta = 2\pi$) is traction free.)

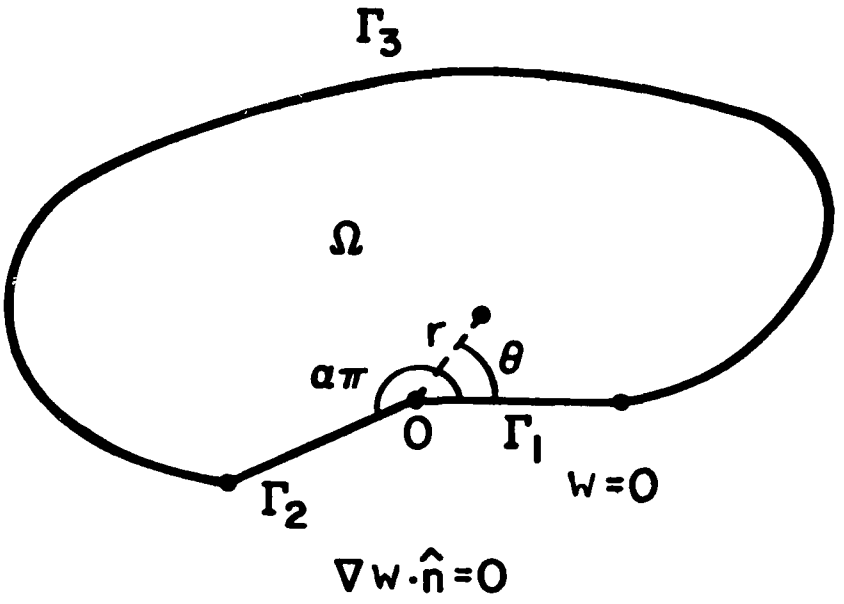

Figure 1.

In a neighborhood of the vertix 0 the solution ω and its derivatives have asymptotic expansions of the form

$$\omega = \sum_{n=1}^{N} k_n r^{(2n-1)\frac{1}{2\alpha}} \sin((2n-1)\frac{\theta}{2\alpha}) + O(r^{(2N+1)\frac{1}{2\alpha}}), \tag{1.4a}$$

$$\nabla\omega = \sum_{n=1}^{N} \frac{2n-1}{2\alpha} k_n r^{(2n-1-2\alpha)\frac{1}{2\alpha}} \begin{pmatrix} \sin((2n-1-2\alpha)\frac{\theta}{2\alpha}) \\ \cos((2n-1-2\alpha)\frac{\theta}{2\alpha}) \end{pmatrix} + O\left(r^{(2N+1-2\alpha)\frac{1}{2\alpha}}\right), \tag{1.4b}$$

for some numbers $k_n, n = 1,\ldots,N$, with N arbitrary. Provided the f_j and g_j's are sufficiently smooth, then in the vicinity of any other vertex, P say, of Ω

$$\omega = O(1)$$

(1.5)

$$\nabla\omega = O(|x-x(P)|^{-3/4})$$

where $|x-x(P)| = [(x_1-x_1(P))^2 + (x_1-x_2(P))^2]^{1/2}$. See [2] for further details. Notice that if $n < \frac{1}{2} + \alpha$, the n^{th} term in the expansion (1.4b) for $\nabla\omega$ is unbounded as $r \to 0$. We can think of the coefficients k_n of these terms as analogs of the stress intensity factors of elasticity. In this paper we generalize this terminology somewhat, and refer to all the coefficients k_n, whether or not the corresponding terms in (1.4) are singular, as stress intensity factors.

Our approach to obtaining approximate values for the "displacement" ω and the "stress" $\frac{\partial\omega}{\partial x_j}$ near 0 will be to first calculate the coefficients k_n by a post-processing of the finite element solution, and then use the asymptotic expansions (1.4) to find the displacement and stresses. Notice that this is a reversal of a "direct" method which is often used to calculate the stress intensity factors: firstly, the finite element solution is "fitted" in some way to (1.4), and the resulting coefficients corresponding to the k_n are taken as the appropriate stress intensity factors.

Although our considerations in this paper will be restricted to the above model problem the ideas of our analysis extend in a natural way to many other two dimensional problems. In particular, everything we do could also be carried out in the context of two dimensional elasticity.

§1.3. Outline of the paper

In §2 and §3 we derive two different expressions for the stress intensity factors k_n. These expressions are both of the general form described by (1.2). Section 4 addresses the accuracy of the post-processed approximations to k_n based on these expressions. Our discussion at this point will be very similar to that in the corresponding section of our earlier paper. Finally, in §5 we give two numerical examples to illustrate the practical effectivity of post-processing in the current context.

§2. The Generalized Influence Function Method

§2.1.

The first method for calculating stress intensity factors that we shall describe is based on an influence function approach. At least in theory, the concept of an influence function for a stress intensity factor has been known for some time (see, for instance, [3]). However, these kinds of ideas do not appear to be widely used in finite element practice (though, see [4],[5] and [10]). Although what we shall say will only be in the context of the model problem (1.3), the ideas may be readily extended to other situations.

§2.2. An expression for k_m

Let φ be a function defined on Ω. For the moment, let us only assume that φ is smooth everywhere in Ω except, perhaps, near the corner of interest at 0. Let P_ℓ ($\ell = 0,\ldots,s-1$) be some enumeration of the vertices of Ω, with P_0 denoting the vertex 0. For $\varepsilon > 0$, sufficiently small, remove from Ω discs of radius ε about each P_ℓ. Denote by Ω_ε the new region so formed. Let $\Gamma_j^{(\varepsilon)}$ and $\gamma_\ell^{(\varepsilon)}$ be as indicated in Figure 2. Multiply (1.3a) by φ and integrate by parts over Ω_ε to obtain

$$(2.1)\quad 0 = \int_{\Omega_\varepsilon} (\nabla^2\omega)\varphi dA = \Big(\sum_\ell \int_{\gamma_\ell^{(\varepsilon)}} + \sum_j \int_{\Gamma_j^{(\varepsilon)}}\Big)(\nabla\omega\cdot\hat{n}\varphi - \nabla\varphi\cdot\hat{n}\omega)ds + \int_{\Omega_\varepsilon} (\nabla^2\varphi)\omega dA,$$

where $\hat{n}$ is the outward pointing unit normal.

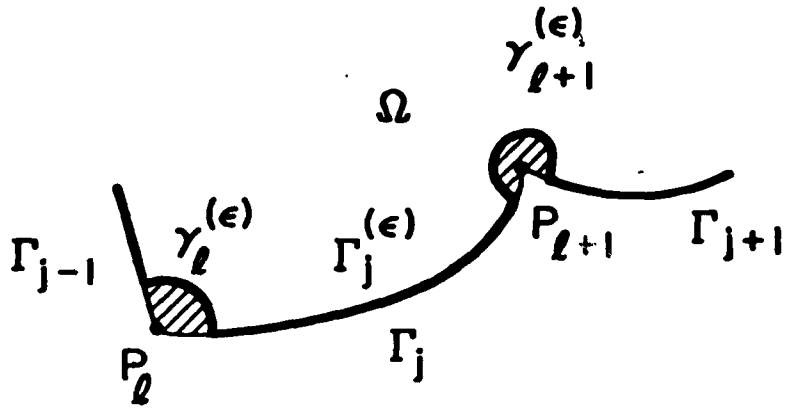

Figure 2.

Now, let us place some further restrictions on φ. Suppose that

(I) $\varphi = 0$ on each of the edges Γ_j to which the Dirichlet boundary condition (1.3b) applies.

(II) In the vicinity of the vertex 0,

$$\varphi = \frac{2}{\pi(2m-1)} r^{(2m-1)\frac{1}{2\alpha}} \sin((2m-1)\frac{\theta}{2\alpha}) + \varphi_b$$

for some $m = 1,2\ldots$ and some smooth function φ_b (bounded second derivatives will suffice).

Using the above properties of φ, along with the expansions (1.4) and (1.5), we may directly evaluate the line integrals over the $\gamma_\ell^{(\varepsilon)}$'s appearing in (2.1). This gives

$$\int_{\gamma_\ell^{(\varepsilon)}} (\nabla\omega\cdot\hat{n}\varphi - \nabla\varphi\cdot\hat{n}\omega)ds = \begin{cases} -k_m + o(1), & \text{if } \ell = 0 \\ o(1), & \text{if } \ell \neq 0. \end{cases}$$

Taking the limit as $\varepsilon \to 0$ in (2.1), and recognizing that $\nabla^2\varphi$

is bounded near 0, leads to the following expression for k_m:

$$(2.2)\quad k_m = \int_\Omega (\nabla^2\varphi)\omega dA + \sum_j^N \int_{\Gamma_j} (g_j\varphi - \nabla\varphi\cdot\hat{n}\omega)ds - \sum_j^D \int_{\Gamma_j} \nabla\varphi\cdot\hat{n}f_j ds,$$

where $\sum_j^N$ and $\sum_j^D$ denote summation over all the edges Γ_j for which the Neumann boundary condition (1.3c) and the Dirichlet boundary condition (1.3b) apply respectively. Notice that if φ had the additional properties

(i) $\nabla^2\varphi = 0$ in Ω, and

(ii) $\nabla\varphi\cdot\hat{n} = 0$ on the edges Γ_j for which the Neumann condition (1.3c) applies,

then (2.2) would become simply

$$(2.3)\quad k_m = \sum_j^N \int_{\Gamma_j} g_j\varphi ds - \sum_j^D \int \nabla\varphi\cdot\hat{n}f_j ds.$$

The function φ could then be thought of as an influence function, relating the applied boundary displacement and traction loading to the resulting stress intensity factor k_m at 0 (see [3]). In general such a φ is not immediately available.

The expression (2.2) is of the form (1.1), and so in line with (1.2) we consider the approximation $\tilde{k}_m$ to k_m calculated using the finite element solution $\tilde{\omega}$,

$$(2.4)\quad \tilde{k}_m = \int_\Omega (\nabla^2\varphi)\tilde{\omega}dA + \sum_j^N \int_{\Gamma_j} (g_j\varphi - \nabla\varphi\cdot\tilde{n}\tilde{\omega})ds - \sum_j^D \int_{\Gamma_j} \nabla\varphi\cdot nf_j ds.$$

Much as in [1], we shall see in §4 that the accuracy of $\tilde{k}_m$ is influenced by the smoothness of $\xi = \nabla^2\varphi$ and $\rho = -\nabla\varphi \cdot \hat{n}$. As before, the issue of how to select a φ for use in (2.4) is essentially a matter of deciding how to satisfy the boundary requirement (I) above in a smooth way. Among others, the cut off function and blending function techniques described in [1] may be used. We shall leave to §5 any further discussion of the actual numerical implementation of (2.4).

§3. The Generalized Energy Release Method

§3.1. Preliminaries

The second approach that we shall discuss is related to the well-known energy release method of fracture mechanics. Over the years this method has been implemented in numerous forms. To name but a few: the J-integral [6,9,10], the stiffness derivative [7] and the crack closure [8,9,10] methods. In common with these methods, the approach that we shall outline in this section only applies to cases where the included angle at the vertex 0 is π or 2π (i.e., $\alpha = 1,2$). This restriction is not too serious since in practice these cases are by far the most important. Again, though we only discuss the model problem (1.3), the technique that we shall outline may be extended to treat other problems.

§3.2. Another expression for k_m

Let φ be a smooth function on Ω (bounded first derivatives on Ω will suffice), and define

$$(3.1)\quad v = \frac{-4\alpha}{\pi(2m-1)(1+2\alpha-2m)}\, r^{(1+2\alpha-2m)\frac{1}{2\alpha}} \sin\!\left((1+2\alpha-2m)\frac{\theta}{2\alpha}\right) \quad (m = 1,2,\ldots).$$

For $\varepsilon > 0$, sufficiently small, and with Ω_ε, $\Gamma_j^{(\varepsilon)}$ and $\gamma_\ell^{(\varepsilon)}$ as in §2.2, consider the integral

$$\Phi_\varepsilon \equiv \int_{\Omega\varepsilon} (\nabla\omega)^T \begin{bmatrix} -\varphi_{,1} & -\varphi_{,2} \\ -\varphi_{,2} & \varphi_{,1} \end{bmatrix} \nabla v\varphi \, dA$$

$$(3.2) \qquad = \left(\sum_\ell \int_{\gamma_\ell^{(\varepsilon)}} + \sum_j \int_{\Gamma_j^{(\varepsilon)}}\right) \begin{bmatrix} -\omega_{,1}{}^{v}{}_{,1} + \omega_{,2}{}^{v}{}_{,2} \\ -\omega_{,1}{}^{v}{}_{,2} - \omega_{,2}{}^{v}{}_{,1} \end{bmatrix} \cdot \hat{n} \, \varphi ds$$

$$- \int_{\Omega_\varepsilon} (-v_{,1} \nabla^2\omega - \omega_{,1} \nabla^2 v) \, dA$$

after an integration by parts. Here $\hat{n}$ denotes the outward pointing unit normal and $(\ )_{,i}$ indicates differentiation with respect to x_i. Since $\nabla^2\omega = 0$ (see 1.3a), and since from (3.1) it is readily verified that $\nabla^2 v = 0$, it follows that the integral over Ω_ε on the right hand of (3.2) vanishes.

Now, let us place some concrete restrictions on φ. Suppose that

(I) $\varphi(0) = 1$, and

(II) $\varphi = 0$ on $\Gamma_3, \Gamma_4, \ldots, \Gamma_s$ (i.e., on all Γ_j's except Γ_1 and Γ_2).

Now introducing the assumption $\alpha = 1,2$, (3.2) becomes

$$\Phi_\varepsilon = \sum_\ell \int_{\gamma_\ell^{(\varepsilon)}} \begin{bmatrix} -\omega_{,1}{}^{v}{}_{,1} + \omega_{,2}{}^{v}{}_{,2} \\ -\omega_{,1}{}^{v}{}_{,2} - \omega_{,2}{}^{v}{}_{,1} \end{bmatrix} \cdot \hat{n} \, \varphi ds.$$

Using (3.1) and the expansions (1.4), (1.5), we may calculate directly

$$\lim_{\varepsilon \to 0^+} \Phi_\varepsilon = k_m.$$

If we assume

(III) In the vicinity of 0, $\nabla\varphi = O(r^{\beta})$ where $\beta > \max(0, \frac{m-\alpha-1}{\alpha})$, then the integrand in the first line of the definition (3.2) of Φ_{ε} is integrable over Ω, and we have

$$(3.3) \qquad k_m = \lim_{\varepsilon \to 0+} \Phi_{\varepsilon} = \int_{\Omega} (\nabla\omega)^T \begin{bmatrix} -\varphi_{,1} & -\varphi_{,2} \\ -\varphi_{,2} & \varphi_{,1} \end{bmatrix} \nabla v \, dA.$$

This is in the form required by (1.1), with

$$\lambda_1 = -\varphi_{,1} v_{,1} - \varphi_{,2} v_{,2}$$

$$\lambda_2 = -\varphi_{,2} v_{,1} + \varphi_{,1} v_{,2},$$

and $\xi = 0$, $\rho = 0$ and $R = 0$.

In accord with (1.2) we may use (2.3) with $\tilde{\omega}$ replacing ω to obtain an approximation $\tilde{k}_m$ to k_m. As usual, in practice we would want λ to be as smooth as possible. One strategy is to let φ be identically 1 in a neighborhood of 0 and then let II be imposed by smooth cut off functions. The condition III is automatically satisfied. This strategy has the advantage of eliminating the need to evaluate a singular integral near 0 (since $\varphi_{,1} = \varphi_{,2} = 0$ there).

It may not at first be apparent what connection the expression (3.3) has with the energy release method. We shall not explain this in detail; however, let us just note two points. Firstly, the matrix

$$\begin{bmatrix} -\varphi_{,1} & -\varphi_{,2} \\ -\varphi_{,2} & \varphi_{,1} \end{bmatrix}$$

can be thought of as a form of stiffness derivative with respect to crack extension. (The function φ characterizes this crack extension.) While secondly the quantity

$$\begin{bmatrix} -\omega_{,1}v_{,1} + \omega_{,2}v_{,2} \\ -\omega_{,1}v_{,2} - \omega_{,2}v_{,1} \end{bmatrix} \cdot \hat{n}$$

which appears in the line integrals of (3.2) can, by formally putting $v = \omega$, be modified to essentially give the integrand of the J_1-integral associated with (1.3),

$$J_1(\Gamma) = \int_\Gamma \frac{1}{2} \begin{bmatrix} -\omega_{,1}^2 + \omega_{,2}^2 \\ -2\omega_{,1}\omega_{,2} \end{bmatrix} \cdot \hat{n} \, ds.$$

§4. The Accuracy of the Approximations $\tilde{k}_m$

Our discussion in this section will be brief, since much of what we said in our earlier paper (see §3.5 of [1]) applies in the current setting also. Pursuing the same argument as there leads, for the techniques of both §2 and §3, to the error relation

$$k_m - \tilde{k}_m = \int_\Omega (\nabla(\omega-\tilde{\omega}))^T \nabla(\psi-\tilde{\psi}) dA \tag{4.1}$$

where ψ and $\tilde{\psi}$ are the exact and finite element solutions of the auxiliary problem,

$$\begin{cases} -\nabla^2\psi = \nabla\cdot\lambda + \xi \quad \text{in} \quad \Omega, \\ \psi = 0 \quad \text{on those } \Gamma_j \text{ for which the Dirichlet condition (1.3b) applies,} \\ \nabla\psi\cdot\hat{n} = \lambda\cdot\hat{n} + \rho \quad \text{on those } \Gamma_j \text{ for which the Neumann condition (1.3c) applies,} \end{cases} \tag{4.2}$$

using the notation of (1.1)/(1.2). (In obtaining (4.1) we have implicitly assumed that the Dirichlet data f_j is exactly representable by a finite element function. If this is not the case, then the expression (4.1) no longer applies. We shall not discuss this situation here.) This auxiliary problem is of the same form as the basic problem (1.3), with only the right hand sides of the differential equation and boundary conditions changed. If we let $E(\cdot)$ denote the strain energy expression associated with the problem (1.3),

$$E(\cdot) = \int_\Omega |\nabla(\cdot)|^2 \, dA,$$

then from (4.1) we obtain the usual estimate

$$(4.3)\quad |k_m-\tilde{k}_m| \le E(\omega-\tilde{\omega})^{1/2}\, E(\psi-\tilde{\psi})^{1/2}$$

$$\le \min_{\nu} E(\omega-\nu)^{1/2} \min_{\nu^*} E(\psi-\nu^*)^{1/2},$$

where ν and ν^* range over all finite element functions which vanish on those Γ_j to which the Dirichlet condition (1.3b) applies.

The conclusion to be drawn from (4.3) is precisely the same as that which we have already noted in [1]: the accuracy of the post-processed value is related to how well the finite element functions are able to approximate both the solution ω of the basic problem and the solution ψ of an auxiliary problem.

The corner points of Ω usually give rise to some form of singular behavior in ω and ψ. This seriously affects how well these functions can be approximated by the finite element functions. Nonetheless, it may be shown, in theory at least, that for suitable "optimally refined" meshes, with p^{th} degree elements $\min_{\nu} E(\omega-\nu)^{1/2} = O(N^{-p/2})$, when N is the number of degrees of freedom of the finite element model. The same meshes also give $\min_{\nu^*} E(\psi-\nu^*)^{1/2} = O(N^{-p/2})$, provided the right hand sides in (4.2) are sufficiently smooth. For such meshes then, we have from (4.3), $|k_m-\tilde{k}_m| = O(N^{-p})$. Of course, from a practical point of view, the constant multiplying the N^{-p} in the $O(N^{-p})$ term is very important. The constant is related amongst other things, to the smoothness of the right hand sides of both the basic problem (1.3) and the auxiliary problem (4.1). A priori, little seems to be able to be said about choosing meshes that optimize its value.

However, on a qualitative level, we again remark on the importance of choosing post-processing procedures with "smooth" λ, ξ and ρ's.

Let us however remark on a point that we shall return to in greater detail in our next paper. Already, by concentrating our attention on the estimate (4.3) we have strayed somewhat from our real objective, which is to find high accuracy approximations to k_m. The actual error in $\tilde{k}_m$ is given by (4.1). An optimal mesh strategy, whether a priori or adaptive, should then be tailored to minimizing the integral in (4.1) rather than the right hand side of the already overly conservative estimate (4.3). The estimate (4.3) assumes the worst possible case, namely that there is no cancellation in the integral (4.1). If there is some cancellation, then $k_m - \tilde{k}_m$ will be overestimated by (4.3).

§5. Some Numerical Examples

§5.1. The FEARS program

The calculations associated with the examples of this section were performed using the FEARS program. FEARS is a research oriented, adaptive finite element package developed at the University of Maryland. A detailed description of the operation and mathematical background of the program can be found in [11]. For the purposes of this paper, the following few remarks will suffice. FEARS assumes that the region under consideration has firstly been partitioned into a number of subregions, each of which is a curvilinear quadrilateral. Within the program, each of these subregions is transformed by a change of coordinates into a unit square. The actual finite element modelling is then carried out on these transformed squares. Square bilinear elements are used. FEARS has an adaptive character: starting from an initial coarse mesh (usually, uniform on each of the transformed squares), the program automatically selects, in a recursive manner, a sequence of "optimal" mesh refinements. The program allows the user some freedom in choosing the criterion on which the "optimality" will be based.

§5.2. Example A: A slit, circular membrane

Let Ω be the unit circle slit along the positive X_1 axis. In the notation of §1.2 let Γ_1 be the upper face of the slit, Γ_2 the lower face of the slit and Γ_3 the circular portion of the boundary of Ω. We consider the following particular case of the model problem (1.3):

$$
\begin{aligned}
\nabla^2\omega &= 0 \quad \text{in } \Omega \\
\omega &= 0 \quad \text{on } \Gamma_1 \\
\frac{\partial\omega}{\partial n} &= 0 \quad \text{on } \Gamma_2 \\
\frac{\partial\omega}{\partial n} &= x_2 \quad \text{on } \Gamma_3.
\end{aligned}
\tag{5.1}
$$

(See Fig. 3). For this problem the expansion (1.4) about the origin takes the form

$$
\omega = k_1 r^{1/4}\sin\frac{\theta}{4} + k_2 r^{3/4}\sin\frac{3\theta}{4} + k_3 r^{5/4}\sin\frac{5\theta}{4} + O(r^{7/4})
$$

$$
\nabla\omega = \frac{k_1 r^{-3/4}}{4}\begin{pmatrix}\sin(-\frac{3}{4}\theta)\\ \cos(-\frac{3}{4}\theta)\end{pmatrix} + \frac{3k_2 r^{-1/4}}{4}\begin{pmatrix}\sin(-\frac{1}{4}\theta)\\ \cos(-\frac{1}{4}\theta)\end{pmatrix} + \frac{5k_3 r^{1/4}}{4}\begin{pmatrix}\sin\frac{\theta}{4}\\ \cos\frac{\theta}{4}\end{pmatrix} + O(r^{3/4}).
\tag{5.2}
$$

Using the method of separation of variables, an infinite series representation of ω may be found. This series can be manipulated to give the following exact values:

$$
E(\omega) = 4.52707,
$$

$$
k_1 = -1.35812, \quad k_2 = .970087, \quad k_3 = .452707
$$

(Note that the influence functions for the k_m are actually readily available in the present case. They are given by

$$
\xi = \frac{2}{\pi(2m-1)}\left(r^{-(2m-1)\frac{1}{2\alpha}} + r^{(2m-1)\frac{1}{2\alpha}}\right)\sin\left((2m-1)\frac{\theta}{2\alpha}\right)
$$

as may be easily verified.)

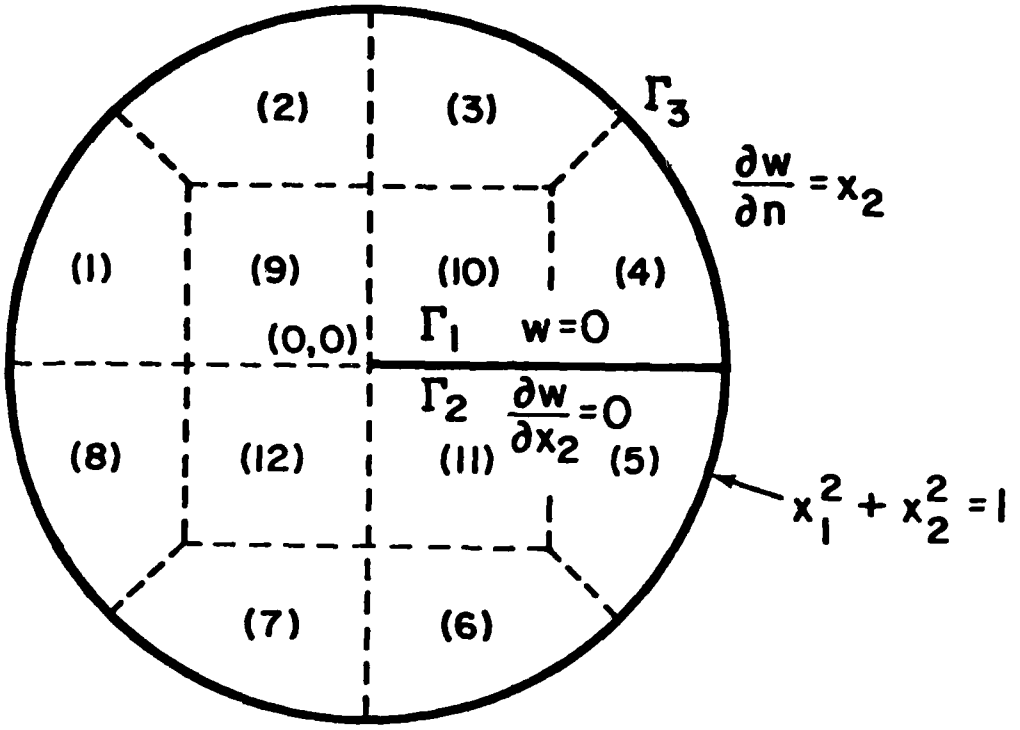

Figure 3.

Table 1 lists some properties of a sequence of four adaptively refined meshes produced by the FEARS program for the problem (5.1) with Ω partitioned as in Figure 3. FEARS was directed in this instance to produce refinements that were "optimal" in the strain energy sense. Note that the mesh I is uniform on each of the transformed squares. Subsequent meshes, exhibit, as would be expected, quite severe refinement about the tip of the slit. Using the approximate solutions corresponding to each of these meshes, we calculate two sets of approximations $\tilde{k}_1$, $\tilde{k}_2$ and $\tilde{k}_3$ to the first three stress intensity factors of (5.2). Firstly, we used the Generalized Influence Function Method of §2 obtained by choosing

No. of Elements (h_{max}/h_{min})	MESH I	MESH II	MESH III	MESH IV
Subregion 1	4(1)	4(1)	4(1)	4(1)
" 2	" "	" "	" "	7(2)
" 3	" "	" "	" "	7(2)
" 4	" "	" "	" "	4(1)
" 5	" "	" "	7(2)	40(2)
" 6	" "	" "	4(1)	10(2)
" 7	" "	" "	" "	13(2)
" 8	" "	" "	" "	4(1)
" 9	" "	10(4)	13(8)	100(64)
" 10	" "	4(1)	19(4)	46(64)
" 11	" "	37(4)	103(32)	145(64)
" 12	" "	25(8)	40(32)	133(256)
Total No. of Elements	48	108	210	513
No. of degrees-of-freedom	56	104	192	447
$E(\tilde{\omega})^{1/2}$	2.02227 (31%)	2.06709 (24%)	2.09383 (18%)	2.11461 (11%)

Table 1. Table of mesh properties for Example A.

(i) h_{max}, h_{min} refer to the maximum and minimum mesh size on each of the transformed squares.

(ii) The quantities in parentheses in the last row are the relative energy norm errors $= \left(\frac{E(\omega-\tilde{\omega})}{E(\omega)} \right)^{1/2}$ for the appropriate meshes.

(iii) The energy norm of the exact solution = $E(\omega)^{1/2} = 2.12769$.

$$\varphi = \frac{2}{\pi(2m-1)} r^{-(2m-1)\frac{1}{4}} \sin((2m-1)\frac{\theta}{4})$$

in (2.2). This gives the expression

$$\tilde{k}_m = \int_{\Gamma_3} (x_2\varphi - \nabla\varphi \cdot \hat{n}\tilde{\omega})ds. \tag{5.3}$$

Notice that for this example the requirement (I) of §2 does not apply to Γ_3. There is no need for us to make φ vanish there. Secondly, we used the Generalized Energy Release Method of §3 with

$$\varphi(x_1,x_2) = \begin{cases} 1 & 0 \le r < \frac{1}{2} \\ 1 - 4(r-\frac{1}{2})^2 & \frac{1}{2} \le r \le 1 \end{cases}$$

in (3.3). This gives the expression

$$\tilde{k}_m = \int_{|r|\ge\frac{1}{2}} \nabla\tilde{\omega} \begin{pmatrix} -\cos\theta & -\sin\theta \\ -\sin\theta & \cos\theta \end{pmatrix} \nabla v(-8(r-\tfrac{1}{2}))dA$$

with v given by (3.1). The results of these computations are displayed in Table 2.

The following conclusions may be drawn from the results shown in Tables 1 and 2.

(a) Despite the presence of singularities at the corner points of Ω, the sequence of adaptively created meshes gives an apparent rate of convergence for the energy norm error in $\tilde{\omega}$ which is close to the theoretically "optimal refinement" rate of $O(N^{-.5})$, where N is the number of degrees-of-freedom of the finite element model. (The II to III refinement step shows an $O(N^{-.47})$ rate and the III to IV step refinement shows an

Mesh	Influence Function Method (% relative error)			Energy Release Method (% relative error)		
	$\tilde{k}_1$	$\tilde{k}_2$	$\tilde{k}_3$	$\tilde{k}_1$	$\tilde{k}_2$	$\tilde{k}_3$
I	-1.164	.9685	.4529	-1.170	.9698	.4528
(31%)	(14.3%)	(.16%)	(.056%)	(13.8%)	(.025%)	(.031%)
II	-1.243	.9718	.4528	-1.249	.9734	.4521
(24%)	(8.5%)	(.17%)	(.026%)	(8.0%)	(.34%)	(.13%)
III	-1.295	.9713	.4532	-1.300	.9726	.4528
(18%)	(4.6%)	(.13%)	(.12%)	(4.3%)	(.26%)	(.011%)
IV	-1.334	.9704	.4533	-1.338	.9700	.4532
(11%)	(1.7%)	(.036%)	(.14%)	(1.5%)	(.012%)	(.11%)
Exact Value	-1.358	.9701	.4527	-1.358	.9701	.4527

Table 2. Table of the computed values of $\tilde{k}_m$ (m=1,2,3) for Example A.

(i) The quantity in parenthesis under each mesh label is the corresponding relative energy norm error = $\left(\frac{E(\omega-\tilde{\omega})}{E(\omega)}\right)^{1/2}$.

(ii) The exact values are correct to the number of significant figures shown.

$O(N^{-.58})$ rate). Had only uniform meshes been used on the transformed squares, theory would have predicted an $O(N^{-.125})$ rate. In that case, to obtain an accuracy in the energy norm comparable to that of the present mesh IV, approximately 3×10^5 degrees-of-freedom would have been required. This would clearly not be a practical proposition.

(b) There seems to be no significant difference between the $\tilde{k}_m$'s calculated using the Influence Function Method and those calculated by the Energy Release Method. Observe that in both cases $\tilde{k}_1$ appears to be converging at a rate twice that of the energy norm error (i.e., at a rate of approximately $O(N^{-1})$). Notice also that the coefficients $\tilde{k}_2$ and $\tilde{k}_3$ are very accurate, even for the relatively coarse meshes I and II. The irregular behavior of the relative error of $\tilde{k}_2$ and $\tilde{k}_3$ as the meshes are refined can probably be attributed, at least partially, to quadrature errors made in the evaluation of the $\tilde{k}_m$. (We used Gaussian quadrature). These coefficients are so accurate that otherwise negligible quadrature errors may now become significant.

It may be shown that the auxiliary functions ψ (see 4.2) corresponding to both the Influence Function Method (5.3) and the Energy Release Method (5.4) all take the form

$$\psi = Cr^{(2m-1)/4} \sin((2m-1)\tfrac{\theta}{4}) \qquad (m = 1,2,3),$$

in the vicinity of the vertex 0. Observe therefore, that the behavior of ψ near 0 becomes more "smooth" as m increases. This will have consequences as regards the approximability of ψ.

Indeed, the poorer accuracy of $\tilde{k}_1$ compared to $\tilde{k}_2$ or $\tilde{k}_3$ can be attributed to this fact.

§5.3. Example B: A slit, square membrane

Let Ω be the square $(-1,1)^2$ which has been slit along the X_1 axis. In the notation of §1.2 let Γ_1 be the upper face of the slit, Γ_2 the lower face of the slit and let $\Gamma_3,\ldots,\Gamma_7$ be some labelling of the remaining straight line segments making up the boundary of Ω. We consider the following particular case of (1.3):

$$
\begin{aligned}
(5.3) \qquad \nabla^2\omega &= 0 \quad \text{on} \quad \Omega \\
\omega &= 0 \quad \text{on} \quad \Gamma_1 \\
\frac{\partial\omega}{\partial n} &= 0 \quad \text{on} \quad \Gamma_2 \\
\omega &= x_2 \quad \text{and} \quad \Gamma_3,\ldots,\Gamma_7.
\end{aligned}
$$

(See Fig. 4). For this problem the expansions (5.2) remain valid about the origin. Using the technique of conformal mappings and the method of separation of variables, an infinite series representation of ω may be found. From this series it can be deduced that

$$k_1 = -.353768, \quad k_2 = .735947, \quad k_3 = .5608491.$$

Unfortunately, this series does not provide an effective means for calculating the exact energy $E(\omega)$ of the exact solution ω.

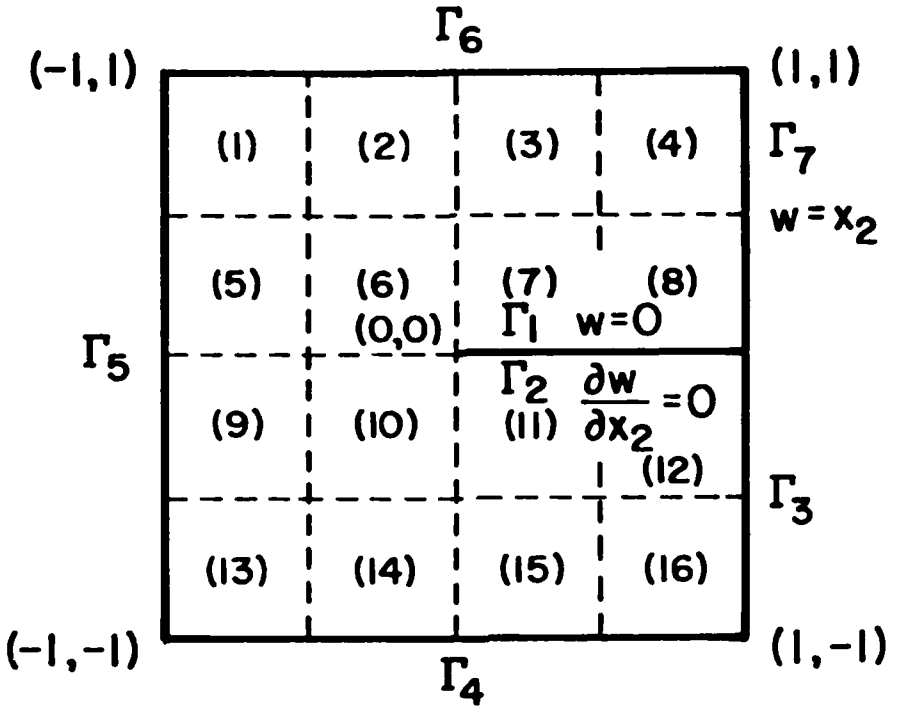

Figure 4.

Table 3 lists some of the characteristics of a sequence of four adaptively refined meshes which were created by FEARS for this problem. The initial partitioning of Ω into subregions is illustrated in Figure 4. FEARS was directed in this instance to produce refinements that were "optimal" in the strain energy sense. Again the first mesh is uniform on each of the transformed squares. The subsequent meshes show, as expected, refinement around the slit tip. Using the approximate solutions corresponding to each of these meshes, we again calculate two sets of approximations $\tilde{k}_1$, $\tilde{k}_2$, $\tilde{k}_3$ to the first three stress intensity factors of (5.2). Firstly, we employ the Generalized Influence Method of §2. In particular we choose

No. of elements (h_{max}/h_{min})	MESH I	MESH II	MESH III	MESH IV
Subregion 1	4(1)	4(1)	4(1)	4(1)
" 2	" "	" "	" "	" "
" 3	" "	" "	" "	" "
" 4	" "	" "	" "	" "
" 5	" "	" "	" "	" "
" 6	" "	" "	67(8)	130(64)
" 7	" "	" "	19(4)	19(4)
" 8	" "	" "	4(1)	4(1)
" 9	" "	" "	4(1)	4(1)
" 10	" "	67(8)	70(8)	91(64)
" 11	" "	34(4)	43(16)	76(16)
" 12	" "	37(4)	40(4)	46(4)
" 13	" "	4(1)	4(1)	4(1)
" 14	" "	" "	" "	" "
" 15	" "	" "	" "	7(2)
" 16	" "	" "	" "	7(2)
Total No. of Elements	64	190	283	412
No. of degrees-of-freedom	48	159	240	348
$E(\tilde{\omega})^{1/2}$	1.93212	1.92293	1.92038	1.91888

Table 3. Table of mesh properties for Example B.

h_{max}, h_{min} refer to the maximum and minimum mesh size on each of the transformed squares.

$$\varphi = X(x_1)X(x_2)\frac{2}{\pi(2m-1)} r^{-(2m-1)\frac{1}{4}} \sin^{(2m-1)\frac{\theta}{4}}$$

where

$$X(t) = \begin{cases} 1 & |t| \le \frac{1}{2} \\ 1 - 4(|t|-\frac{1}{2})^2 & |t| > \frac{1}{2} \end{cases}$$

in (2.2). Notice that in contrast to the corresponding choice in Example A, we here had to require that $\varphi = 0$ on the non-slit part of $\partial\Omega$. We have done this by using the cut off function $X(x_1)X(x_2)$. The expression used to evaluate $\tilde{k}_m$ is the particular form of (2.2)

$$\tilde{k}_m = \int_\Omega \nabla^2\varphi\tilde{\omega}dA - \sum_{j=3}^{7} \int_{\Gamma_j} \nabla\varphi \cdot \hat{n}x_2 ds.$$

The second set of approximations is based on the Generalized Energy Release Method of §3 with the function φ of (3.3) given by

$$\varphi(x_1,x_2) = \bar{\varphi}(x_1)\bar{\varphi}(x_2),$$

where

$$\bar{\varphi}(t) = \begin{cases} 1 & 0 \le |t| < \frac{1}{2} \\ 1 - 2(|t| - \frac{1}{2}) & \frac{1}{2} \le |t| \le 1 \end{cases}$$

The results of these computations are displayed in Table 4.

Just as in Example A, we see that for this example there are no significant differences in accuracy between the influence function and energy release methods. We also see here the high accuracy of $\tilde{k}_2$ and $\tilde{k}_3$ even for the coarse meshes I and II. Note also that the convergence of $\tilde{k}_1$ is consistent with the $O(N^{-1})$ rate that we would have for a theoretically optimal refinement.

Mesh	Influence Function Method (% relative error)			Energy Release Method (% relative error)		
	$\tilde{k}_1$	$\tilde{k}_2$	$\tilde{k}_3$	$\tilde{k}_1$	$\tilde{k}_2$	$\tilde{k}_3$
I	-.4309 (22%)	.7400 (.56%)	.5602 (.12%)	-.4203 (19%)	.7361 (.024%)	.5627 (.33%)
II	-.3941 (11%)	.7364 (.067%)	.5605 (.053%)	-.3924 (11%)	.7357 (.032%)	.5610 (.029%)
III	-.3750 (6.0%)	.7364 (.068%)	.5607 (.033%)	-.3748 (6.0%)	.7361 (.020%)	.5609 (.015%)
IV	-.3671 (3.8%)	.7363 (.052%)	.5607 (.027%)	-.3669 (3.7%)	.7359 (.0071%)	.5610 (.027%)
Exact Value	-.3538	.7359	.5608	-.3538	.7359	.5608

Table 4. Table of computed values of $\tilde{k}_m$ (m = 1,2,3) for Example B.

The exact values are correct to the number of significant figures shown.

§5.4. Conclusions

For these examples we see that the use of post-processing techniques allied with an appropriate adaptive mesh selection algorithm, makes it possible to obtain the leading stress intensity factor with say a five-percent accuracy, while using only a moderate number of degrees-of-freedom in the finite element model (around 250 for our examples). This, even though the strain energy norm error for such a mesh may still be of the order of 20% (as in Example A). This latter observation also shows the importance of being specific when speaking of the accuracy of a finite element solution - a solution giving acceptable accuracy for one quantity, may not be acceptable for another.

Bibliography

[1] I. Babuška, A. Miller, The Post-Processing Approach in the Finite Element Method, Part 1: Calculation of Displacements, Stresses and other Higher Derivatives of the Displacements, submitted to International Journal of Numerical Methods in Engineering.

[2] P. Grisvard, Boundary Value Problems in Non-Smooth Domains, University of Maryland, Department of Mathematics, Lecture Notes No. 19, 1980.

[3] M. Š. Birman, G. E. Skvorcov, On the square integrability of the highest derivatives of the solution of the Dirichlet problem on domains with piecewise smooth boundaries (In Russian), Izvestija Vyšich Učebnych Zavedenij, Math. 1962 No. 5, pp. 12-21.

[4] M. Dobrowolski, Numerical Approximation of Elliptic Interface and Corner Problems, Habilitationsschrift, University of Bonn, 1981.

[5] H. Blum, A Simple and Accurate Method for the Determination of Stress Intensity Factors and Solutions for Problems on Domains with Corners, in The Mathematics of Finite Elements and Applications IV, MAFELAP, 1981, Ed. J. R. Whiteman, Academic Press, London, 1982.

[6] J. R. Rice, A Path Independent Integral and Approximate Analysis of Strain Concentration by Notches and Cracks, Journal of Applied Mechanics, Vol. 35, 1968, pp. 379-386.

[7] D. M. Parks, A Stiffness Derivative Finite Element Technique for Determination of Crack Tip Stress Intensity Factors, International Journal of Fracture, Vol. 10, No. 4, 1974, pp. 487-502.

[8] T. K. Helen, On the Method of Virtual Crack Extensions, International Journal of Numerical Methods in Engineering, Vol. 9, No. 1, 1975, pp. 187-207.

[9] E. M. Morozov, G. P. Nikišhkov, The Finite Element Method in Fracture Mechanics (in Russian), Nauka, Moscow, 1980.

[10] Computational Fracture Mechanics, Proceedings of ASME 2nd National Congress on Pressure Vessels and Piping (San Francisco, June, 1975), Ed. E. F. Rybicki, S. E. Benzley, ASME, New York, 1975.

[11] C. Mesztenyi, W. Szymczak, FEARS User's Manual, Technical Note No. BN-991, 1982, Institute for Physical Science and Technology, University of Maryland.

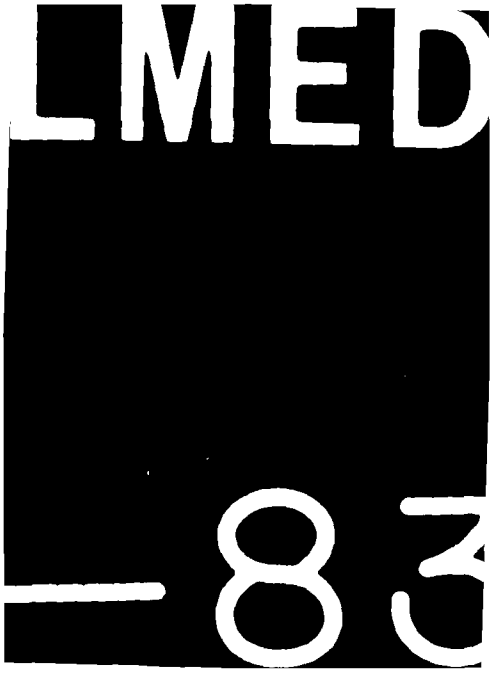
LMED
-83